

Influence of water-rock interaction on the pH and heavy metals content of groundwater during in-situ oil shale exploitation

Shu-ya Hu^(a,b,c), Chang-Lai Xiao^(b,c), Xiu-Juan Liang^{(b,c)*}, Yu-qing Cao^(b,c)

- (a) Environmental Science and Engineering, Qingdao University, Qingdao 266071, China
- (b) Key Laboratory of Groundwater Resources and Environment of Ministry of Education, Jilin University, Changchun 130021, China
- (c) College of New Energy and Environment, Jilin University, Changchun 130021, China

Abstract. *In this paper, step-by-step groundwater-rock interaction experiments were performed to investigate the migration of heavy metals (Pb, Cr, Zn) into the water and the pH change of oil shale and oil shale ash aqueous solutions (hereinafter OS solution and OSA solution, respectively) during the in-situ production of oil shale. For geochemical calculations the PHREEQC software was used to simulate pH variation in the aqueous solutions at different temperatures and CO₂ partial pressures (P_{CO_2}). The pH of most solutions was between 6.95 and 7.49 and changed significantly with increasing reaction time. The simulated data were closest to the experimental results at $P_{CO_2} = 10^{-2}$. A clear effect of reaction temperature and pH on the Pb content in the aqueous solutions was observed. The Pb content in the OSA solution was 0.36–0.47 µg/L, being higher than that in the OS solution (0.13–0.26 µg/L). The Cr content in OS and OSA solutions was from 0.55 to 0.70 µg/L. The Zn content in the OS solution was 1.17–3.61 µg/L, being significantly influenced by reaction temperature.*

Keywords: *oil shale in-situ exploitation, water-rock interaction, heavy metals, groundwater.*

1. Introduction

Owing to the increasing global demand for liquid fuels, unconventional petroleum resources are playing an important role in the world's energy portfolio today [1]. Oil shale is a natural, fine-grained, laminated black or brown combustible material. It consists of kerogen, a complex organic material with a high molecular weight, which is finely distributed in an inorganic matrix [2–6]. Oil is neither readily separated nor extracted from oil shale; common extraction methods include retorting, combustion and liquefaction [7].

* Corresponding author: e-mail 90shuya@sina.com

The processing of oil shale is generally carried out using two methods: (i) above-ground (ex-situ) processing to extract oil from mined shale; and (ii) underground (in-situ) processing in whose case heating is applied to extract oil via wells. Ex-situ processing requires oil shale to be mined beforehand. Oil shale ash, a by-product of the traditional ex-situ processing, is considered a serious environmental hazard [3]. In in-situ processing heating is applied to oil shale without removing it from the ground. It has been argued that in-situ mining has great potential; hence, oil shale sites suitable for in-situ processing are being explored and appropriate technologies developed [8, 9].

Oil shale is a fossil fuel similar to coal, but with a higher mineral content [10]. In addition to the main elements (C, H, N, O), oil shale contains trace heavy metals, such as Cr, Cd and Pb [11]. During the in-situ processing of oil shale, the fracturing water, pyrolysis water and groundwater flowing into the oil shale layer interact with both oil shale and the solid oil shale pyrolysis residue (ash) which remains after the in-situ oil generation and extraction. The wastewater resulting from the oil shale retorting process contains significant amounts of oil, sulfides, volatile phenols and potentially toxic heavy metals [12]. Heavy metals can cause great harm to ecosystems, especially the groundwater [13]. At the same time, there are very few studies on the mobility of heavy metals such as Pb, Cr and Zn during oil shale exploitation. Yan et al. [6] investigated the interaction between kerogen and various metals during the pyrolysis and combustion of oil shale and found that heavy metals increased the reactivity of organic matter in oil shale. Bai et al. [14] discovered that Cu, Pb, Zn and Cr were present in the oil shale bottom slag in trace concentrations, but mainly in the form of a stable residue or bound in sulfides.

The in-situ processing of oil shale requires a long heating time; for example, Shell's in-situ conversion process (ICP) utilises electricity to heat oil shale underground over the period of two years [15]. Although the whole oil shale utilisation process adversely affects the environment, groundwater included, yet to date, the effect of its in-situ conversion processing on the groundwater has not been fully clarified. In order to study the migration of heavy metals and the pH change of the aqueous solution during the in-situ production of shale oil, a series of water-rock interaction experiments using oil shale and water, and oil shale ash and water were conducted. In addition, pH changes in the oil shale and oil shale ash aqueous solutions (hereinafter OS solution and OSA solution, respectively) under different reaction conditions were simulated.

2. Material and methods

2.1. Water-rock interaction tests

The oil shale sample used in this study was obtained from an exposed oil shale section located in Nong'an city, China, which has approximately 16.8 billion

tons of industrial reserves. The sampled oil shale is found in Quaternary (Holocene, Q_4^{al}) alluvial-lacustrine deposits composed of mudstone and sandstone interlayered with oil shale. On average, the oil yield of oil shale was from 5.0 to 12.1%, the calorific value 3.38–8.17 MJ/kg, the ash content 77.71–94.48% and the TOC 7.87–14.16 mg/g [16]. The oil shale sample was dried in an oven at 110 °C for 4 h before weighing. Oil shale and oil shale ash were both ground and passed through a 20-mesh sieve to a particle size less than 1 mm. Then, 1 L of deionized water was added to 100 g of the prepared oil shale samples. The solid-liquid mixtures were placed in a water bath, and various reaction temperatures and times were used in the water-rock interaction experiments. The reaction temperatures were 20 ± 0.1 , 50 ± 0.1 , 80 ± 0.1 and 100 ± 0.1 °C, and the reaction times were 0.5, 1, 2, 5, 8, 15, 20 and 30 days. A total of 36 oil shale aqueous solutions (OS solutions) were prepared. The solutions were shaken and filtered after the reactions were complete. Then oil shale was heated to 400 °C by using a tube furnace under nitrogen gas to obtain oil shale ash. The above-described method was also applied to prepare oil shale ash aqueous solutions (OSA solutions) for water-rock interaction experiments.

The contents of heavy metals Pb, Cr and Zn in the aqueous solutions were determined, besides, the pH of the aqueous solutions was also measured. For pH measurement a P33-pH/ORP pH meter was employed. A Shimadzu AA-6000CF flame atomic absorption (FAA) spectrophotometer (limit of detection (LOD) = 0.003–0.120 µg/L) was used to determine metal contents in the aqueous solutions [17].

2.2. Forward hydrogeochemical modeling

In the in-situ pyrolysis process of oil shale, water-rock interactions are quite complex and the reaction cycle is long. Depending on the exploitation method, the chemical component contents of oil produced in the retorting process are different because of the secondary conversion of shale oil and gas during the in-situ processing of oil shale. Therefore, such conditions cannot be completely replicated under laboratory conditions. However, suitable results can be obtained over a shorter time period using computer simulations. PHREEQC, a hydrogeochemical simulation software package developed by the U.S. Geological Survey [18], was used for modelling the laboratory leaching test and simulating a leaching scenario [19]. This software can simulate the equilibrium between aqueous solutions and minerals, calculate the pH of a solution, and perform simulation calculations at different temperatures. We simulated the equilibrium values for oil shale-water reactions at different temperatures and CO_2 partial pressures (P_{CO_2}).

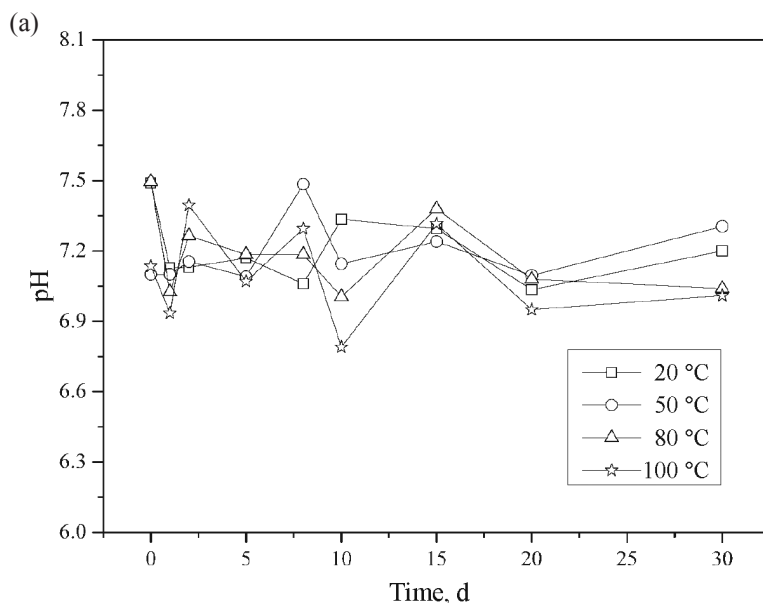
2.3. X-ray diffraction analysis method

The X-ray diffraction (XRD) method is used to analyze the qualitative mineral composition of oil shale. Oil shale was ground and sieved with 200 mesh screens for further XRD analysis on a D-MAX 2200 X-ray powder crystal diffractometer (Rigaku, Japan). The device's operating parameters were as follows: incident light source Cu K α radiation, Ni slice filtering, the 2 θ resolution 0.05° and the scanning range 0–90°.

3. Results

3.1. pH of aqueous solutions

Figure 1 shows the changes in the pH of OS and OSA solutions at different reaction temperatures. It is revealed that the solutions' pH did not change much at different temperatures. The pH of the OS solution was between 6.95 and 7.49 at all temperatures, only in the experiment at 100 °C it dropped to 6.80 on the 10th day. The pH of the OS solution varied less with increasing reaction time compared to the OSA solution. The pH of the latter varied somewhat more, from 6.68 to 7.95, with both increasing reaction time and temperature, and after 20 days was stabilized at different reaction temperatures. After 30 days of reaction, the pH was the highest at 20 °C, at which point the OSA solution was slightly alkaline. After 30 days at 100 °C, the pH of the OS solution was 7.01 and that of the OSA solution 7.02, both values being close to the neutral.



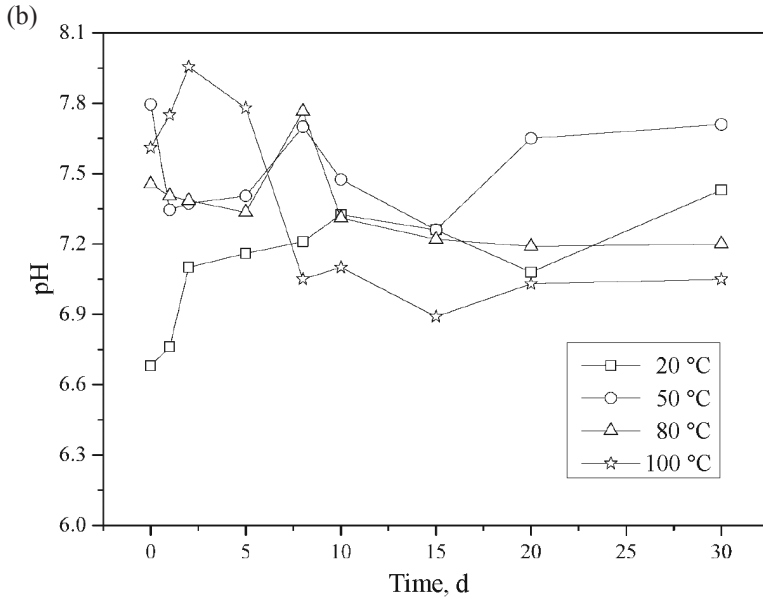


Fig. 1. Temperature-dependent pH curves as a function of time for (a) OS aqueous solutions and (b) OSA aqueous solutions.

To assess the change of solution pH during the in-situ retorting the modeling approach was applied. The maximum P_{CO_2} generated by pyrolysis of 100 g of Nong'an oil shale in a closed environment was 0.0857 [20]. In addition, the buried depth of the oil shale layer is relatively great, and the CO_2 generated in the formation during the in-situ exploitation mainly comes from the dissolved amount of the fracturing fluid, which is much lower than that in the vadose zone. Therefore, the selected reaction conditions used in the simulation were as follows: P_{CO_2} 10^{-1} , 10^{-2} , 10^{-3} , 10^{-4} and 10^{-5} MPa, and temperatures 20, 50, 80, 100, 150, 200, 250 and 300 °C. As in the lab experiments, the reactants were 1 L of distilled water and 100 g of Nong'an oil shale. The simulation results under equilibrium conditions are shown in Figure 2.

The simulation results showed that at temperatures below 200 °C the pH of the solution was greatly influenced by P_{CO_2} , decreasing with the increase of the latter. At temperatures above 200 °C, the effect of P_{CO_2} on pH was negligible. From 20 to 150 °C, the solution pH was relatively stable with increasing temperature, decreasing slightly and then increasing, as most curves show. The simulated results were most similar to the experimental data at $P_{\text{CO}_2} = 10^{-2}$. At this value of P_{CO_2} , the simulated balance pH values were 7.55, 7.35, 7.39, 7.45, 7.74, 8.52, 8.71 and 7.86 at temperatures of 20, 50, 80, 100, 150, 200, 250 and 300 °C, respectively.

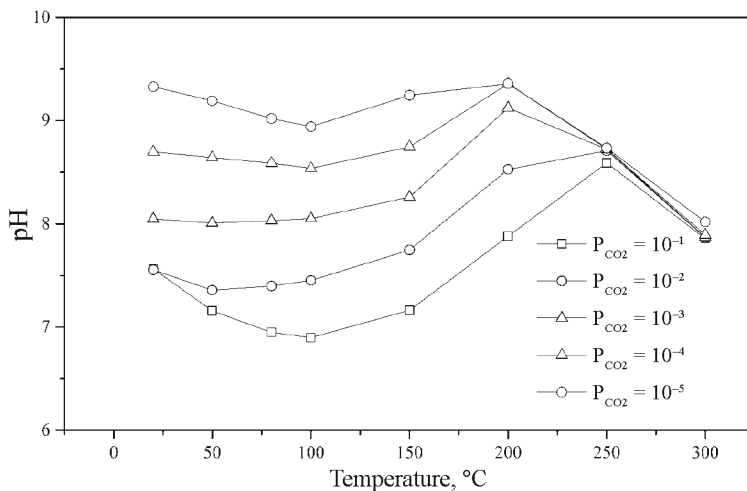


Fig. 2. Simulated temperature-dependent pH curves for OS aqueous solutions at different CO_2 partial pressures.

3.2. Heavy metal contents in aqueous solutions

The heavy metal contents of oil shale and oil shale ash used in the experiments are given in the Table.

Table. Heavy metal concentrations in oil shale and oil shale ash

Sample	Pb, $\mu\text{g/g}$	Cr, $\mu\text{g/g}$	Zn, $\mu\text{g/g}$
Oil shale	27.90 ± 0.69	36.39 ± 0.38	65.61 ± 1.18
Oil shale ash	22.73 ± 0.31	32.62 ± 1.06	62.44 ± 1.26

Figure 3 shows the Pb content in the OS and OSA aqueous solutions under different reaction conditions. Initially, the Pb content in the OS solution increased with increasing reaction time, then stabilized after 10 days of reaction. After 30 days at 100, 80, 50 and 20 °C, the Pb content in the OS solution was 0.26, 0.19, 0.17 and 0.13 $\mu\text{g/L}$, respectively. At 100, 80 and 50 °C, the trend of change in the Pb content of the OSA solution over time was similar to that of the OS solution. At 20 °C, the initial Pb content in the OSA solution was 0.45 $\mu\text{g/L}$. With increasing reaction time, the content of Pb decreased, reaching equilibrium after 15 days of reaction. After 30 days at 100, 80, 50 and 20 °C, the Pb content in the OSA solution was 0.47, 0.44, 0.38 and 0.36 $\mu\text{g/L}$, respectively. None of these values exceeded the standards for drinking water quality in China.

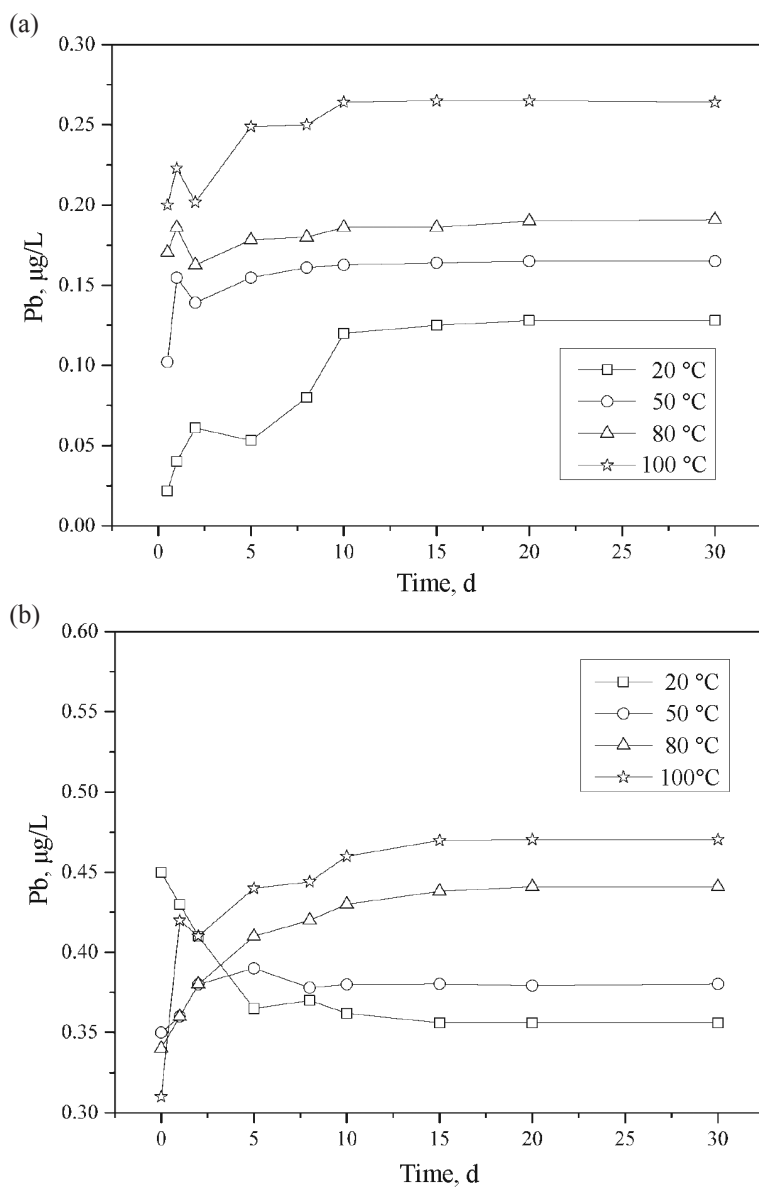


Fig. 3. Temperature-dependent Pb content as a function of time in (a) OS aqueous solutions and (b) OSA aqueous solutions.

Figure 4 shows the Cr content in the aqueous solutions of oil shale and oil shale ash under different reaction conditions. The Cr content in the OS solution did not change significantly with increasing reaction time and was within the range of 0.55–0.65 $\mu\text{g/L}$. The reaction temperature also had a little effect on

the Cr content in the solutions. At 100, 80, 50 and 20 °C, the average Cr contents in the OS solution were 0.59, 0.60, 0.60 and 0.60 $\mu\text{g/L}$, respectively. In contrast, the Cr content in the OSA solution first increased at the initial stage of the reaction and then decreased rapidly. For example, at 100 °C, the Cr content of 0.60 $\mu\text{g/L}$ was measured on the first day, which increased to 0.70 $\mu\text{g/L}$ by the fifth day. However, the Cr content remained stable at 0.59–0.60 $\mu\text{g/L}$ after 10 days.

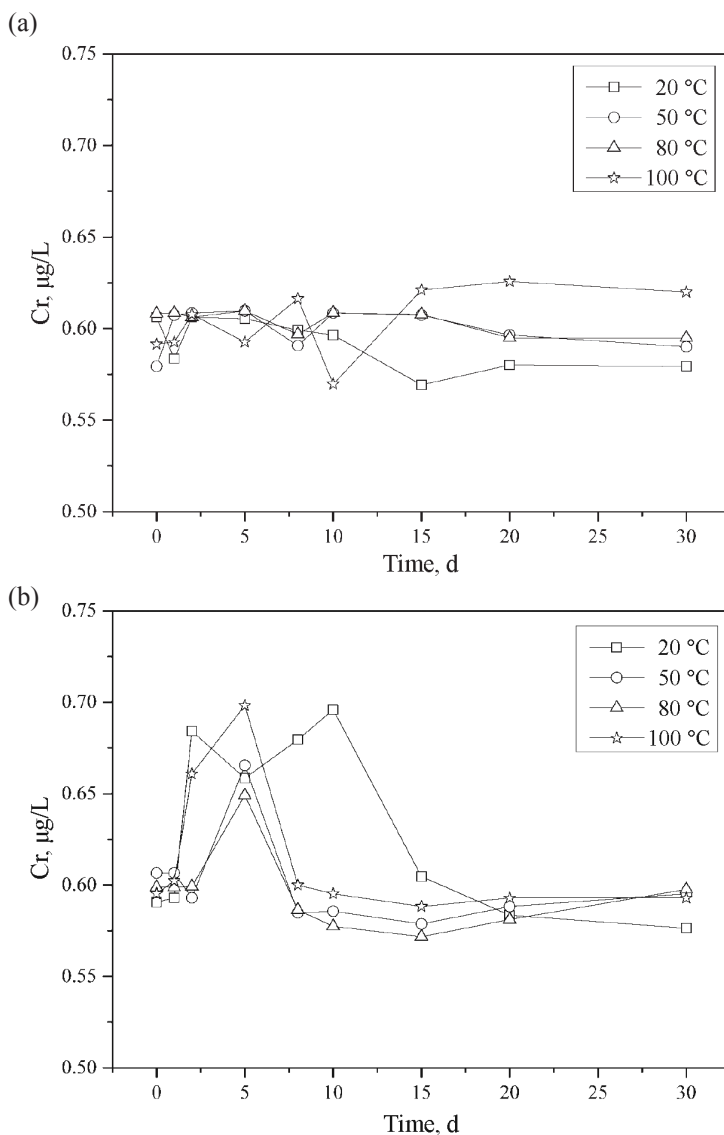


Fig. 4. Temperature-dependent Cr content as a function of time in (a) OS aqueous solutions and (b) OSA aqueous solutions.

Figure 5 shows the content of Zn in the aqueous solutions of oil shale and oil shale ash under different reaction conditions. The Zn content in the OS solution ranged from 1.17 to 3.61 $\mu\text{g/L}$. The reaction temperature had a great influence on the content of Zn in the solution, which averaged 2.86, 2.67, 1.94 and 1.40 $\mu\text{g/L}$ at 100, 80, 50 and 20 $^{\circ}\text{C}$, respectively. With increasing reaction time, the Zn content in the OS solution increased gradually. In the OSA solution, the content of Zn ranged from 0.01 to 0.31 $\mu\text{g/L}$. No clear trend of the increase of Zn content with increasing reaction temperature was observed. However, with increasing reaction time, the Zn content tended to first increase and then decrease.

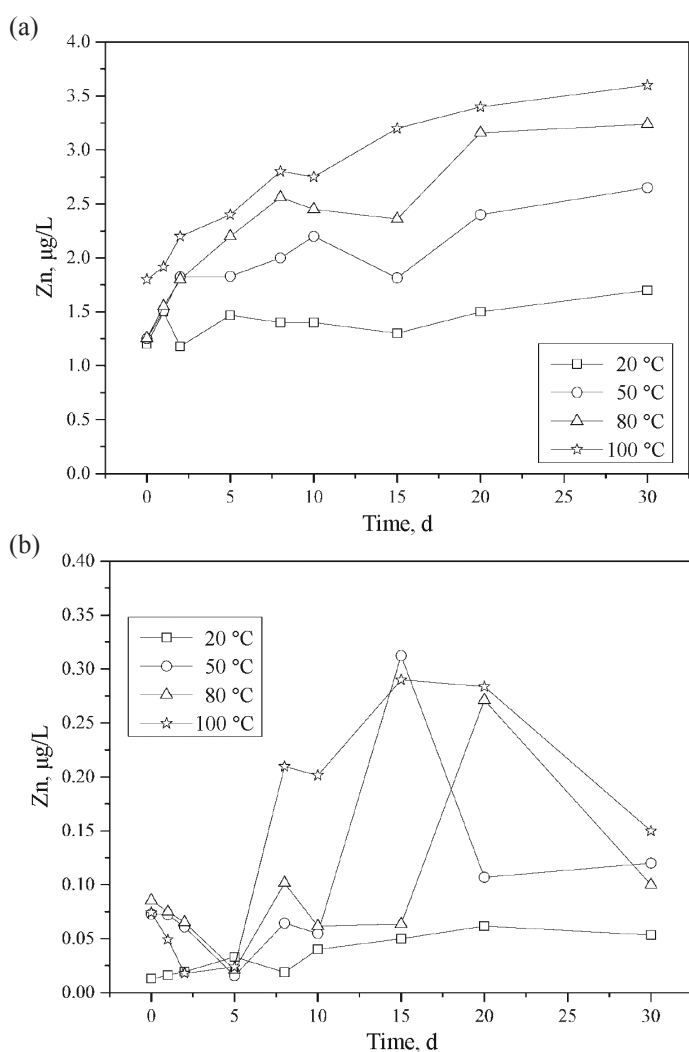


Fig. 5. Temperature-dependent Zn content as a function of time in (a) OS aqueous solutions and (b) OSA aqueous solutions.

4. Discussion

4.1. pH changes in aqueous solutions

The pH value of an aqueous solution is an important variable that affects both the surface charges of the adsorbent and the degree of ionization and speciation of the adsorbate during the adsorption process [21]. The XRD analysis of Nong'an oil shale (Fig. 6) showed its dominant mineral phases to be plagioclase, pyrite, quartz, calcite and dolomite, with minor amounts of illite. Calcite and dolomite are carbonate minerals, quartz is a silicate mineral, and illite and plagioclase are aluminosilicate minerals. These inorganic minerals hydrolyze to form large amounts of OH^- , which increases the pH of aqueous solutions.

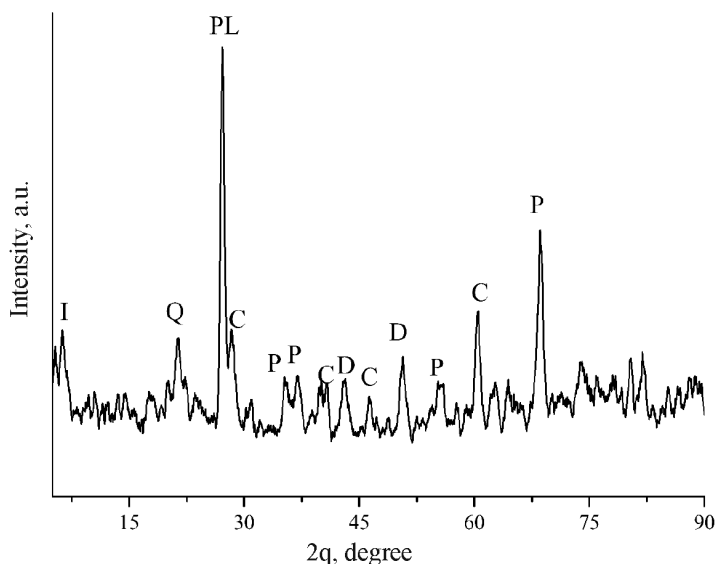
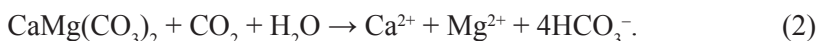
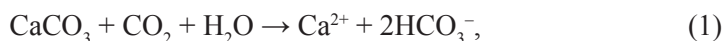
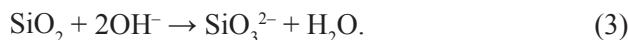


Fig. 6. XRD pattern of oil shale. Abbreviations: I – illite, Q – quartz, PL – plagioclase, C – calcite, P – pyrite, D – dolomite. Cu K α radiation.

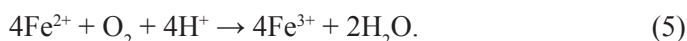
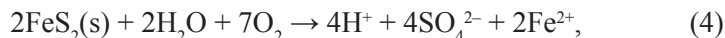
The interaction between carbonate and water is mainly controlled by the dissolution and precipitation of calcite and dolomite. P_{CO_2} in the reaction system controls the dissolution and precipitation of these two minerals. When CO_2 is involved in the reaction, the dissolution of carbonate is as follows:



The dissolution of dolomite and calcite will consume CO_2 and produce a large amount of HCO_3^- , during which the latter further hydrolyzes to form OH^- , which increases the pH of the solution. Since oil shale pyrolysis releases a large amount of water, along with oil and gas components, higher contents of individual inorganic minerals are present in oil shale ash compared with oil shale under the same reaction conditions. Therefore, the pH of the OSA solution was higher than that of the OS solution after 30 days of reaction. Oil shale pyrolysis produces CO_2 and forms H_2CO_3 in aqueous solutions. H_2CO_3 dissociates in water to neutralize the alkaline solution. Hence, the variation of the pH of the OS solution with both time and temperature was less significant. Hydrolysis of silicate minerals forms silicic acid; however, as both the solubility of quartz and the degree of dissociation of silicic acid are very low, the effect of this process on the solution pH is low. Though, in alkaline environments, the solubility of quartz increases dramatically:



In addition, the pyrite content in oil shale also affects the pH of its aqueous solution. Pyrite was oxidized by dissolved oxygen in the OS aqueous solution to form H_2SO_4 and Fe^{2+} , furthermore the latter was oxidized to Fe^{3+} as shown in Equations (4) and (5):



However, due to the low content of dissolved oxygen and temperature limitation, the effect of this process was insignificant.

Oil shale contains aluminosilicate minerals such as illite and plagioclase. Hydrolysis of these minerals affords silicic acid, alkali compounds and secondary minerals. The reaction is generally written as follows:

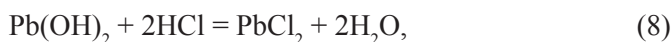
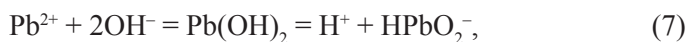


where M is K^+ , Na^+ , Ca^{2+} , Mg^{2+} or another cation.

The hydrolysis of aluminosilicate minerals is extremely slow. Although the pH of the aqueous solution is not changed significantly, the newly formed secondary minerals adhere to the surface of the primary rock particles, forming a strongly alkaline microenvironment on it. Kovda [22] showed that after hydrolysis of aluminum silicate the solution pH was slightly alkaline, 9–10. These conditions can accelerate the hydrolysis of silicate minerals, further increasing the pH (alkalinity).

4.2. Heavy metals release

The chemical state of metallic elements determines their solubility in water [23]. Metal elements in oil shale and oil shale ash may exist in various forms: water soluble, ion exchange, combined carbonate and sulfide, organic combination, and residual state. The Pb content in the aqueous solution of rock mainly depends on the content of soluble Pb in it. In the rock aqueous solution Pb appears in two reaction states: water solubility equilibrium and complexation equilibrium. There are different Pb^{2+} hydroxides present in the aqueous solution of rock; hence, pH also affects its Pb content [24]. Lead hydroxides can ionize H^+ or OH^- in the solution and interact with both acids and bases:



In our experiments, the Pb content in the reaction solution increased under both acidic and alkaline conditions. On the first day of reaction, the OSA solution was acidic and its Pb content relatively high. As the reaction progressed, the solution neutralized and the Pb content gradually decreased. Pb and its compounds are volatile at high temperatures and the vapor of Pb can be in a highly dispersed aerosol state [24] and can be adsorbed on the oil shale ash surface. Therefore, the Pb content in the OSA solution was higher than that in the OS solution. Meanwhile, the solubility of Pb in the latter solution was affected by the solubility of PbCl_2 , PbF_2 , PbSO_4 , PbCO_3 and PbS [25].

In solution chromium may have four ionic forms (Cr^{3+} , CrO_4^{2-} , CrO_4^{2-} and $\text{Cr}_2\text{O}_7^{2-}$) whose trivalent and hexavalent states are the most common. Trivalent chromium is less soluble in water than the hexavalent state, is easily adsorbed and has low mobility. In acidic solutions, trivalent chromium can form complexes with negatively charged substances, such as hydroxyl complexes, and migrate in complex form. Hexavalent chromium is relatively stable in alkaline solutions and it has high solubility and mobility. Although trivalent chromium is toxic, it is far less toxic than hexavalent chromium. Under certain conditions, trivalent and hexavalent chromium can be converted into each other. Trivalent chromium is highly hydrolytic and can be oxidized under alkaline conditions. Under reducing conditions, hexavalent chromium will be converted into trivalent chromium to form $\text{Cr}(\text{OH})_3$ precipitates. In our experiments, the initial Cr content in the OSA solution was high and then decreased over time, probably owing to hexavalent chromium ions (e.g., CrO_4^{2-}) in solution being reduced by organic compounds to trivalent chromium and forming sediments.

Zn, which is insoluble in pure water but can dissolve in alkaline solutions, is usually present in aqueous solutions in the divalent form. Zinc can easily be hydrolyzed to form polyhydroxyl complexes and can undergo complexation

reactions with inorganic complexants such as Cl^- , SO_4^{2-} , CO_3^{2-} and HCO_3^- [26]. Zn can also be complexed with organic complexants, such as amino acids and organic acids, and used in combination. The complexation of hydroxyl with Zn^{2+} can greatly improve the solubility of zinc oxide, which can be adsorbed by inorganic and organic colloids. Shendrika and Faudel [27] analyzed the metal contents in the western Colorado oil shale and its pyrolysis oil, gas and water after processing. The pyrolytic water contained mainly oxides and semimetallic B, as well as Cu, while As and Zn were the main metals in the oil and exhaust gas. Other metals, such as Be, Cd, Cr, Co, Pb, Mn, Hg, Mo, Ni and Se, remained in the oil shale ash. The varying content of Zn in the OSA solution may have been caused by the discharge of Zn in oil shale with the pyrolysis oil and gas, resulting in a lower content of soluble Zn. With increasing reaction time and temperature, the organic content in the OS solution increased, which allowed complexation with Zn, resulting in its higher content. However, the pyrolysis of organic matter increases the contact area between oil shale and water and accelerates the dissolution of Zn.

5. Conclusions

For the first time, the influence of in-situ oil shale exploitation on the pH of and heavy metal contents in oil shale and oil shale ash aqueous solutions was studied using laboratory tests and numerical simulations. Hydrolysis of carbonate and silicate minerals increases the alkalinity of oil shale aqueous solutions. The pH of the oil shale aqueous solution varied less than that of the oil shale ash aqueous solution with increasing reaction time and its dependence on reaction temperature was quite insignificant. The simulated pH values were the closest to the experimental values at $P_{\text{CO}_2} = 10^{-2}$ MPa. The Pb and Zn contents in the oil shale aqueous solution increased with increasing reaction temperature, but a similar effect on Cr was not observed. In the oil shale ash aqueous solution, only the Pb content increased with increasing reaction temperature. The Cr content in the oil shale ash aqueous solution first increased and then decreased rapidly with increasing reaction time. Owing to the highly dispersed aerosol state, Pb can be adsorbed on the surface of oil shale ash, which results in its higher content in the OSA aqueous solution compared to that of OS.

Acknowledgements

This work was supported by the National Natural Science Foundation of China (Grant No. 41572216), the China Geological Survey Bureau Shenyang Geological Survey Center (Grant No. 121201007000150012), and the Provincial School Co-construction Project Special-Leading Technology Guide (Grant No. SXGJQY2017-6).

REFERENCES

1. Saif, T., Lin, Q., Bijeljic, B., Blunt, M. J. Microstructural imaging and characterization of oil shale before and after pyrolysis. *Fuel*, 2017, **197**, 562–574.
2. Häsänen, E., Aunela-Tapola, L., Kinnunen, V., Latjava, K., Mehtonen, A., Salmikangas, T., Leskelä, J., Loosaar, J. Emission factors and annual emissions of bulk and trace elements from oil shale fueled power plants. *Sci. Total Environ.*, 1997, **198**(1), 1–12.
3. Luan, J., Li, A., Su, T., Li, X. Translocation and toxicity assessment of heavy metals from circulated fluidized-bed combustion of oil shale in Huadian, China. *J. Hazard. Mater.*, 2009, **166**(2–3), 1109–1114.
4. Blinova, I., Bityukova, L., Kasemets, K., Ivask, A., Käkinen, A., Kurvet, I., Bondarenko, O., Kanarbik, L., Sihtmäe, M., Aruoja, V., Schvede, H., Kahru, A. Environmental hazard of oil shale combustion fly ash. *J. Hazard. Mater.*, 2012, **229–230**, 192–200.
5. Jefimova, J., Irha, N., Reinik, J., Kirso, U., Steinnes, E. Leaching of polycyclic aromatic hydrocarbons from oil shale processing waste deposit: A long-term field study. *Sci. Total Environ.*, 2014, **481**, 605–610.
6. Yan, J., Jiang, X., Han, X., Liu, J. A TG–FTIR investigation to the catalytic effect of mineral matrix in oil shale on the pyrolysis and combustion of kerogen. *Fuel*, 2013, **104**, 307–317.
7. Pimentel, P. M., Oliveira, R. M. P. B., Melo, D. M. A., Anjos, M. J., Melo, M. A. F., González, G. Characterization of retorted shale for use in heavy metal removal. *Appl. Clay Sci.*, 2010, **48**(3), 375–378.
8. Khan, N. A., Engle, M. A., Dungan, B., Omar Holguin, F., Xu, P., Carroll, K. C. Volatile-organic, molecular characterization of shale-oil-produced water from the Permian Basin. *Chemosphere*, 2016, **148**, 126–136.
9. Maaten, B., Loo, L., Konist, A., Nešumajev, D., Pihu, T., Külaots, I. Decomposition kinetics of American, Chinese and Estonian oil shales kerogen. *Oil Shale*, 2016, **33**(2), 167–183.
10. Al-Otoom, A. Y., Shawabkeh, R. A., Al-Harashsheh, A. M., Shawaqfeh, A. T. The chemistry of minerals obtained from the combustion of Jordanian oil shale. *Energy*, 2005, **30**(5), 611–619.
11. Ge, Y. Z., Liu, W. F., Li, F., Gong, Y. L., Hu, L. A survey on speciation analysis of typical heavy metals in different spatial levels, *Journal of Nanchang Institute of Technology*, 2016, **35**(6), 11–15 (in Chinese).
12. Al-Harashsheh, S., Al-Ayed, O., Amer, M., Moutq, M. Analysis of retorted water produced from partial combustion of Sultani oil shale. *J. Environ. Protect.*, 2017, **8**(9), 1018–1025.
13. Farkas, A., Erratico, C., Viganò, L. Assessment of the environmental significance of heavy metal pollution in surficial sediments of the River Po. *Chemosphere*, 2007, **68**(4), 761–768.
14. Bai, J. R., Wang, Q., Chen, Y., Xu, C. H., Chen, D. F. Study on heavy metals leaching toxicity of fly ash and bottom slag from oil shale CFB. *Chinese Journal of Environmental Engineering*, 2010, **4**(8), 1892–1896 (in Chinese).

15. Brandt, A. R. Converting oil shale to liquid fuels: Energy inputs and greenhouse gas emissions of the Shell in situ conversion process. *Environ. Sci. Technol.*, 2008, **42**(19), 7489–7495.
16. Liu, Z. J., Yang, H. L., Dong, Q. S., Zhu, J. W., Guo, W., Ye, S. Q., Liu, R., Meng, Q. T., Zhang, H. L., Gan, S. C. *Oil Shale in China*. Petroleum Industry Press, Beijing, 2009 (in Chinese).
17. Hu, S. Y., Xiao, C. L., Jiang, X., Liang, X. J. Potential impact of in-situ oil shale exploitation on aquifer system. *Water*, 2018, **10**, 649.
18. Parkhurst, D. L., Appelo, C. A. J. *User's Guide to PHREEQC (Version 2) – A Computer Program for Speciation, Batch-Reaction, One-Dimensional Transport, and Inverse Geochemical Calculations*. U.S. Geological Survey, Water-Resources Investigations Report 99-4259, 1999. 10.3133/wri994259.
19. Tiruta-Barna, L. Using PHREEQC for modelling and simulation of dynamic leaching tests and scenarios. *J. Hazard. Mater.*, 2008, **157**(2–3), 525–533.
20. Qiu, S. W. *Experimental Study on the Impacts of Oil Shale in-situ Pyrolysis on Groundwater Hydrochemical Characteristics*. Doctoral Dissertation, Jilin University, 2016 (in Chinese).
21. Bao, W. W., Zou, H. F., Gan, S. C., Xu, X. C., Ji, G. J., Zheng, K. Y. Adsorption of heavy metal ions from aqueous solutions by zeolite based on oil shale ash: Kinetic and equilibrium studies. *Chem. Res. Chinese U.*, 2013, **29**(1), 126–131.
22. Kovda, V. A. Biosphere, soil cover and their changes. In: *Science Technology and the Future* (Velikhov, E. P., Gvishiani, J. M., Mikulinsky, S. R., eds.), 1980, 397–410.
23. Migliavacca, D. M., Teixeira, E. C., Gervasoni, F., Conceição, R. V., Rodriguez, M. T. R. Metallic elements and isotope of Pb in wet precipitation in urban area, South America. *Atmos. Res.*, 2012, **107**, 106–114.
24. Schincariol, R. A., Rowe, R. K. Contaminant hydrogeology. In: *Geotechnical and Geoenvironmental Engineering Handbook* (Rowe, R. K., ed.), Boston, MA, 2001.
25. Li, S. Y., Bai, J. R., Chen, Y., Wang, Q., Guan, X. H. Study on the volatility of lead during pyrolysis of oil shale. *Journal of Fuel Chemistry and Technology*. 2008, **36**(4), 489–493 (in Chinese).
26. Liao, Z. J. *Pollution Hazards and Migration Transformation of Trace Heavy Metal Elements in the Environment*. Science Press, Beijing, 1989 (in Chinese).
27. Shendrikar, A. D., Faudel, G. B. Distribution of trace metals during oil shale retorting. *Environ. Sci. Technol.*, 1978, **12**(3), 332–334.

Presented by V. Lahtvee, K. Kirsimäe

Received March 26, 2019